

# Low frequency Rabi spectroscopy of dissipative two level systems. The dressed state approach.

Ya. S. Greenberg

*Novosibirsk State Technical University, 20 K. Marx Ave., 630092 Novosibirsk, Russia.*

(Dated: October 27, 2018)

We have analyzed a dissipative two level quantum system (TLS) which is continuously and simultaneously irradiated by a high and low frequency excitation. The interaction of the TLS with a high frequency excitation is considered in the frame of the dressed state approach. A linear response of the coupled TLS and corresponding photon field system to a signal whose frequency is of the order of the Rabi frequency is found. The response exhibits undamped low frequency oscillations, whose amplitude has a clear resonance at the Rabi frequency with the width being dependent on the damping rates of the TLS. The method can be useful for low-frequency Rabi spectroscopy in various physical systems described by a two-level Hamiltonian, such as nuclei spins in NMR, double well quantum dots, superconducting flux and charge qubits, etc. The application of the method to a superconducting flux qubit and to the detection of NMR is considered in detail.

PACS numbers: 74.50.+r, 84.37.+q, 03.67.-a

## I. INTRODUCTION

It is well known that under resonant irradiation a quantum two-level system (TLS) can undergo coherent (Rabi) oscillations. The frequency of these oscillations is proportional to the amplitude of the resonant field<sup>1</sup> and is much lower than the gap frequency of the TLS. This effect is widely used in molecular beam spectroscopy<sup>2</sup>, and in quantum optics<sup>3</sup>. During the last few years it has been proved experimentally that Rabi spectroscopy can serve as a valuable tool for the determination of relaxation times in solid-state quantum mechanical two-level systems, qubits, which are to be used for quantum information processing<sup>4</sup>. Normally, these systems are strongly coupled to the environment, which results in the fast damping of the Rabi oscillations. It prevents the use of conventional continuous measurements schemes for their detection, although special schemes for the detection of coherent oscillations through a weak continuous measurement of a TLS were proposed in<sup>5,6,7</sup>. Consequently, Rabi oscillations are measured by using a pulse technique which harnesses the statistics of switching events of the occupation probability between two energy levels with the excitation and readout being taken at the gap frequency of the TLS, which normally lies in the GHz range<sup>8,9,10,11</sup>.

Recent successful development of the method of low frequency characterization of flux qubits by weak continuous measurements in the radio frequency domain (see review paper<sup>12</sup> and references therein) allowed the first spectroscopic monitoring of Rabi oscillations with a low-frequency tank circuit which had been tuned to the Rabi frequency of the flux qubit<sup>13</sup>. These experiments stimulated theorists to study different methods for the detection of Rabi oscillations involving low frequency (compared to the energy gap between the two levels) electronic circuitry<sup>14,15,16,17</sup>.

One of the methods for the detection of Rabi resonance at low frequencies has been suggested in papers<sup>18,19</sup>. The

method involves irradiating a TLS continuously and simultaneously by two external sources. The first source with frequency  $\omega_0$ , which is close to the energy gap between the two levels, excites the low-frequency Rabi oscillations. Normally, Rabi oscillations are damped out with a rate, which depends on how strongly the system is coupled to the environment. However, if a second low-frequency source is applied simultaneously to the TLS it responds with persistent low frequency oscillations. The amplitude of these low-frequency oscillations has a resonance at the Rabi frequency and its width is dependent on the damping rates of the system. In papers<sup>18,19</sup> we analyzed the effect in the frame of Bloch equations for the quantities  $\langle\sigma_Z\rangle$ ,  $\langle\sigma_Y\rangle$ ,  $\langle\sigma_X\rangle$ , where the brackets denote the averaging over the environmental degrees of freedom. Two external sources at high and low frequency were incorporated in the structure of Bloch equations from the very beginning. We showed analytically as well as by direct computer simulations of the Bloch equations that the quantities  $\langle\sigma_Z\rangle$ ,  $\langle\sigma_Y\rangle$ ,  $\langle\sigma_X\rangle$  exhibit undamped oscillations with a resonance at the Rabi frequency.

The present paper differs from<sup>18,19</sup> in that here we study the problem within a dressed state approach, which is well known in quantum optics<sup>20</sup>. This approach has a great advantage over the method used in<sup>19</sup>. In that paper the effect appeared purely mathematically as the solution of the nonlinear Bloch equations for the averaged quantities, which are not quantum in their nature. It was not clear whether the effect had a quantum nature or it was a consequence of nonlinear structure of Bloch equations.

By using the dressed state approach we show here that the effect has definitely a quantum nature. From the Heisenberg quantum equations of motion we derive the Bloch like equations for the elements of the reduced density matrix and find the low frequency susceptibilities of the TLS coupled to a photon field. We show that, as distinct from the cases in quantum optics, in dissipative solid state TLS there exists an interaction which can induce transitions between the dressed Rabi levels. These

transitions result in the low frequency response of the system, with the resonance being at the Rabi frequency. In addition, the dressed state approach allowed us to find important contribution to slow dynamics which comes from the transitions between the levels which are spaced apart by the gap frequency  $\omega_0$ . This contribution is described by the low frequency dynamics of  $\kappa$  matrix elements (see below), and it cannot be obtained within the approach used in<sup>19</sup>. Another advantage of the dressed state approach is that the expressions we obtain for low frequency susceptibility for two level system have a rather general nature and can be applied for the investigation of specific physical systems. As an illustration of our approach in the paper we study in detail two rather different physical systems: the flux qubit and real spin under NMR conditions. Our approach allows us also to obtain some interesting results which could not be obtained within the method used in<sup>19</sup>. For example, we show that the population of Rabi levels becomes inverted under high frequency irradiation, that can lead to the heating of the low frequency source as was shown in Section 7A for the resonant tank of the flux qubit.

The paper is organized as follows. In Section II, for the sake of the completeness we give a brief overview of a TLS interacting with a one mode laser field which is tuned to the gap of the TLS. The structure of the energy levels of the global system (TLS and associated laser field) consists of manifolds where the spacing between the two levels in a given manifold is equal to the Rabi frequency. We write down the wave functions for these two levels and calculate the transition amplitudes between them which result from the low frequency excitation. In Section III we define the density matrix in an uncoupled basis and write down the phenomenological rate equations for the elements of the density matrix. In Section IV the elements of the reduced density matrix (the density matrix traced over the photon number  $N$ ) are defined, and the Bloch like rate equations for the elements of the reduced density matrix are derived. For the case of small high frequency detuning the steady state solutions to these equations are found. It is shown that under high frequency irradiation the population of the Rabi levels becomes inverted. In Section V the Bloch equations for the reduced density matrix are modified to include the low frequency excitation. The linear low frequency susceptibilities for the response of the coupled TLS and associated photon field system to a low frequency excitation are found in Section VI both for arbitrary and small high frequency detuning. Two important applications of the method (superconducting flux qubit and NMR spins) are considered in detail in Section VII.

## II. INTERACTION OF A TLS WITH A LASER FIELD IN THE FRAME OF DRESSED STATES. A BRIEF OVERVIEW

We start with the Hamiltonian of a TLS subjected to a high frequency field:

$$H = \frac{\Delta}{2}\sigma_x + \frac{\varepsilon}{2}\sigma_z + \hbar\omega_0(a^\dagger a + 1/2) + H_{int} \quad (1)$$

Here the first two terms describe an isolated TLS, which can be used to model a great variety of situations in physics and chemistry: from a spin-(1/2) particle in a magnetic field to superconducting flux and charge qubits<sup>4,21</sup>. In order to be exact we use the TLS in (1) to describe a double-well system where only the ground states of the two wells are occupied, with  $\Delta$  being the energy splitting of a symmetric ( $\varepsilon = 0$ ) TLS due to quantum tunnelling between two wells. The quantity  $\varepsilon$  is the bias, the external energy parameter which makes the system asymmetric. The third term in (1) is the Hamiltonian of the laser mode,  $a^\dagger$  and  $a$  being the creation and annihilation operators. The last term in (1) describes the interaction of the TLS with a laser field. This interaction modulates the energy asymmetry between the two wells:

$$H_{int} = -\frac{1}{2}\sigma_z F(a^\dagger + a) \quad (2)$$

The Hamiltonian of the TLS in (1) is written in the localized state basis, i.e. in the basis of states localized in each well. In terms of the eigenstates basis, which we denote by upper-case subscripts for the Pauli matrices  $\sigma_X$ ,  $\sigma_Y$ , and  $\sigma_Z$ , Hamiltonian (1) reads as:

$$H = \frac{\Delta_\varepsilon}{2}\sigma_Z + \hbar\omega_0(a^\dagger a + 1/2) + H_{int} \quad (3)$$

where  $\Delta_\varepsilon = \sqrt{\Delta^2 + \varepsilon^2}$  is the gap between the two energy states and

$$H_{int} = \frac{1}{2} \left( \frac{\Delta}{\Delta_\varepsilon} \sigma_X - \frac{\varepsilon}{\Delta_\varepsilon} \sigma_Z \right) F(a^\dagger + a) \quad (4)$$

First, we consider a noninteracting system which involves the TLS and a laser field. The system is described by the Hamiltonian:

$$H_0 = \frac{\Delta_\varepsilon}{2}\sigma_Z + \hbar\omega_0(a^\dagger a + 1/2) \quad (5)$$

We denote the ground state and excited state wave functions of the TLS as  $|a\rangle$  and  $|b\rangle$ , respectively, where they have properties:  $\sigma_Z|a\rangle = -|a\rangle$ ,  $\sigma_Z|b\rangle = |b\rangle$ ,  $\sigma_X|a\rangle = |b\rangle$ ,  $\sigma_X|b\rangle = |a\rangle$ . The eigenfunctions of the photon field are  $|N\rangle$ :  $a^\dagger|N\rangle = \sqrt{N+1}|N+1\rangle$ , and  $a|N\rangle = \sqrt{N}|N-1\rangle$ . We denote the eigenfunctions of the noninteracting TLS and associated photon system as a tensor product  $|a, N\rangle \equiv |a\rangle \otimes |N\rangle$ , and  $|b, N\rangle \equiv |b\rangle \otimes |N\rangle$ . Up to a constant term the energies of these states are:

$$H_0|a, N\rangle = \left( -\frac{\Delta_\varepsilon}{2} + \hbar\omega_0 N \right) |a, N\rangle \quad (6)$$

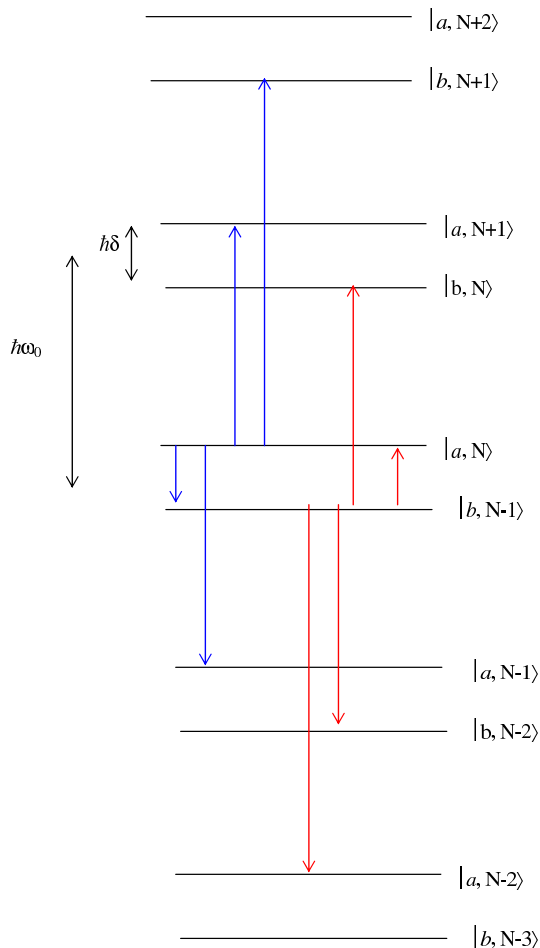


FIG. 1: (Color online). Levels of the noninteracting TLS and associated photon field system. The level spacing in a given manifold is  $\hbar\delta$ . The spacing between neighboring manifolds is  $\hbar\omega_0$ . The red (blue) arrows show the transitions induced by  $H_{int}$  from the state  $|b, N-1\rangle$  ( $|a, N\rangle$ ).

$$H_0|b, N\rangle = \left(\frac{\Delta_\varepsilon}{2} + \hbar\omega_0 N\right)|b, N\rangle \quad (7)$$

For a photon frequency  $\omega_0$  close to the TLS frequency  $\Delta_\varepsilon/\hbar$  and a small detuning  $\delta = \omega_0 - \Delta_\varepsilon/\hbar \ll \omega_0, \Delta_\varepsilon/\hbar$ , where for definitiveness we assume  $\delta > 0$ , it is seen from (6) and (7) that the energies of the states  $|a, N+1\rangle$  and  $|b, N\rangle$  are close to each other:  $E_{a, N+1} - E_{b, N} = \hbar\delta$ . The same is true for the pairs of states  $|a, N\rangle$  and  $|b, N-1\rangle$ ,  $|a, N+2\rangle$  and  $|b, N+1\rangle$ , and so on. Therefore, the energy levels of the system under consideration is a ladder of pairs of manifolds which are specified by the photon number  $N$  (see Fig. 1). Every manifold is parameterized by a pair of states with a small spacing between them,  $\hbar\delta$ , and the distance between neighboring manifolds is equal to the photon energy,  $\hbar\omega_0$ .

This ladder of manifolds is quite similar to the one for atom-field interactions<sup>20</sup>. However, a principal difference is the structure of the interaction Hamiltonian (4).

In quantum optics there is no "longitudinal" interaction between an atomic spin and photon field which is proportional to  $\sigma_Z$ . It is the presence of this bias interaction in a dissipative TLS that leads to some effects which are not observed in quantum optics.

It should be considered now how these levels are modified due to the interaction with (4). For a pair of these closed spacing levels within a given manifold,  $|a, N\rangle$ ,  $|b, N-1\rangle$  interaction (4) causes a transition between them with the amplitude

$$\langle a, N|H_{int}|b, N-1\rangle = \frac{\Delta F}{2\Delta_\varepsilon}\sqrt{N} \quad (8)$$

Therefore, within 2D Hilbert space the wave functions  $|a, N\rangle$  and  $|b, N-1\rangle$  are mixed to give new wave functions for the dressed states  $|1, N\rangle$ , and  $|2, N\rangle$ :

$$|1, N\rangle = \sin\theta|a, N\rangle + \cos\theta|b, N-1\rangle \quad (9)$$

$$|2, N\rangle = -\cos\theta|a, N\rangle + \sin\theta|b, N-1\rangle \quad (10)$$

where we define the state with higher energy as  $|1, N\rangle$ .

The form of Eqs. (9) and (10) ensures the normalization and orthogonality of the wave functions  $|1, N\rangle$  and  $|2, N\rangle$ , which are eigenfunctions of Hamiltonian (3). Accordingly, the uncoupled states  $|a, N\rangle$ ,  $|b, N-1\rangle$  can be expressed in terms of the dressed states  $|1, N\rangle$ ,  $|2, N\rangle$ :

$$|a, N\rangle = \sin\theta|1, N\rangle - \cos\theta|2, N\rangle \quad (11)$$

$$|b, N-1\rangle = \cos\theta|1, N\rangle + \sin\theta|2, N\rangle \quad (12)$$

By using standard quantum mechanical techniques we can find the eigenenergies and the angle  $\theta$ :

$$E_\pm = \frac{1}{2}(E_{|a, N\rangle} + E_{|b, N-1\rangle}) \pm \frac{1}{2}\hbar\Omega_R \quad (13)$$

where the upper (lower) sign corresponds to  $|1, N\rangle$  ( $|2, N\rangle$ ). The quantity  $\Omega_R$  in (13) is the Rabi frequency<sup>22</sup>

$$\Omega_R = \sqrt{\delta^2 + \Omega_1^2} \quad (14)$$

where  $\Omega_1 = \Delta F/\hbar\Delta_\varepsilon$ , and  $\sqrt{N}$  is incorporated in the high frequency amplitude  $F$ .

For the angle  $\theta$  we obtain  $\tan 2\theta = -\Omega_1/\delta$ , where  $0 < 2\theta < \pi$ , so that  $\cos 2\theta = -\delta/\Omega_R$ ,  $\cos\theta = \frac{1}{\sqrt{2}}\left(1 - \frac{\delta}{\Omega_R}\right)^{1/2}$ , and  $\sin\theta = \frac{1}{\sqrt{2}}\left(1 + \frac{\delta}{\Omega_R}\right)^{1/2}$ .

When the interaction is switched off ( $F \rightarrow 0$ ) then, as would be expected, the state  $|1, N\rangle$  tends to  $|a, N\rangle$ , and the state  $|2, N\rangle$  tends to  $|b, N-1\rangle$ . Therefore, by taking into account the interaction between the TLS and the photon field the level structure of a given manifold looks like that shown in Fig. 2. The interaction results in an increase of the energy gap between the states  $|a, N\rangle$

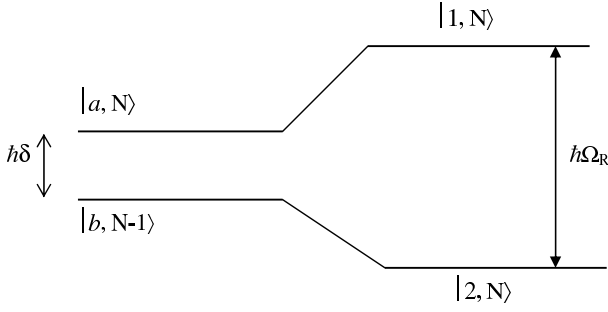


FIG. 2: The level structure of a dressed manifold. The uncoupled states  $|a, N\rangle$  and  $|b, N-1\rangle$  are transformed by the interaction between the TLS and photon field into the two dressed states  $|1, N\rangle$  and  $|2, N\rangle$ .

and  $|b, N-1\rangle$ . Consequently, it is said that these states are dressed by the interaction. From now on we will call these two nearby dressed states Rabi levels.

Up to now the picture has been quite similar to that known from atom-photon interactions<sup>20</sup>. However, a drastic difference appears if we consider the excitation of the dressed levels  $|1, N\rangle$  and  $|2, N\rangle$  by a signal the frequency of which is comparable with Rabi frequency  $\Omega_R$ . Such a low frequency signal cannot change the number  $N$  of high frequency photons, therefore, in quantum optics the transition between these two states is not allowed since, in the language of quantum optics, the atom dipole operator is transversal: it is proportional to  $\sigma_X$ . Therefore, the atom dipole operator connects only the levels, say  $|a, N\rangle$  and  $|b, N\rangle$ , which belong to the different manifolds.

In the TLS the transitions between nearby states  $|1, N\rangle$  and  $|2, N\rangle$  are caused by the "longitudinal" term in the interaction Hamiltonian, which is proportional to  $\sigma_Z$ . Let us assume that system (1) additionally interacts with the low frequency signal  $G \cos \omega t$ , so that the term  $-\sigma_z G \cos \omega t$  is added to Hamiltonian (1), where the frequency  $\omega$  is of the same order of magnitude as the Rabi frequency  $\Omega_R$ . In the eigenbasis this low frequency Hamiltonian is transformed as follows:

$$H_{int}^{LF} = \left( \frac{\Delta}{\Delta_\varepsilon} \sigma_X - \frac{\varepsilon}{\Delta_\varepsilon} \sigma_Z \right) G \cos \omega t \quad (15)$$

The transitions between the Rabi levels  $|1, N\rangle$  and  $|2, N\rangle$  are caused by the second term in the brackets of (15):

$$\langle 1, N | H_{int}^{LF} | 2, N \rangle = -\frac{\varepsilon G \Omega_1}{\Delta_\varepsilon \Omega_R} \quad (16)$$

In what follows we show that these transitions result in the undamped low frequency oscillations of the populations of initial levels  $|a\rangle$  and  $|b\rangle$  which can be detected by using appropriate electronic circuitry.

### III. RATE EQUATIONS FOR THE DENSITY MATRIX IN UNCOUPLED BASIS

The elements of the density matrix  $\sigma$  in the basis of the uncoupled levels  $|a, N\rangle$  and  $|b, N\rangle$  are defined as follows:

$$\begin{aligned} \sigma_{aa}^{NN'} &= \langle a, N | \sigma | a, N' \rangle \\ \sigma_{bb}^{NN'} &= \langle b, N | \sigma | b, N' \rangle \\ \sigma_{ab}^{NN'} &= \langle a, N | \sigma | b, N' \rangle \end{aligned} \quad (17)$$

Since the spontaneous transitions between the levels  $|a\rangle$  and  $|b\rangle$ , which lead to their decay do not change the photon numbers the rate equations for the density matrix  $\sigma$  can be written in the following form:

$$\frac{d\sigma_{bb}^{NN'}}{dt} = -\frac{i}{\hbar} (E_{bN} - E_{bN'}) \sigma_{ab}^{NN'} - \sigma_{bb}^{NN'} \Gamma_\downarrow + \sigma_{aa}^{NN'} \Gamma_\uparrow \quad (18)$$

$$\frac{d\sigma_{aa}^{NN'}}{dt} = -\frac{i}{\hbar} (E_{aN} - E_{aN'}) \sigma_{ab}^{NN'} - \sigma_{aa}^{NN'} \Gamma_\uparrow + \sigma_{bb}^{NN'} \Gamma_\downarrow \quad (19)$$

$$\frac{d\sigma_{ab}^{NN'}}{dt} = -\frac{i}{\hbar} (E_{aN} - E_{bN'}) \sigma_{ab}^{NN'} - \sigma_{ab}^{NN'} \Gamma_\varphi \quad (20)$$

where  $\Gamma_\downarrow$  is the transition rate from the state  $|b, N\rangle$  to state  $|a, N\rangle$  (relaxation rate),  $\Gamma_\uparrow$  is the transition rate from the state  $|a, N\rangle$  to state  $|b, N\rangle$  (excitation rate), and the quantity  $\Gamma_\varphi$  is the rate of decoherence. For equilibrium conditions the relaxation and excitation rates are related by the detailed balance law:

$$\Gamma_\uparrow = \Gamma_\downarrow \exp\left(-\frac{\Delta_\varepsilon}{k_B T}\right) \quad (21)$$

From (21) we obtain

$$\Gamma_- T_1 = -\tanh\left(\frac{\Delta_\varepsilon}{2k_B T}\right) \quad (22)$$

where we define  $\Gamma_- = \Gamma_\uparrow - \Gamma_\downarrow$  and the longitudinal relaxation time  $T_1^{-1} = \Gamma_\uparrow + \Gamma_\downarrow$ .

The equations (18), (19), and (20) can be written in the operator form:

$$\frac{d\sigma}{dt} = -\frac{i}{\hbar} [H_0, \sigma] + \hat{L} \quad (23)$$

where the Hamiltonian of the uncoupled system  $H_0$  is given in (5). The operator  $\hat{L}$  is defined by its matrix

elements which follows from (18), (19) and (20):

$$\begin{aligned}
\widehat{L} = & -\Gamma_{\downarrow} \sum_{N_1, N_2} |bN_1\rangle\langle bN_1|\sigma|bN_2\rangle\langle bN_2| \\
& + \Gamma_{\uparrow} \sum_{N_1, N_2} |bN_1\rangle\langle aN_1|\sigma|aN_2\rangle\langle bN_2| \\
& - \Gamma_{\uparrow} \sum_{N_1, N_2} |aN_1\rangle\langle aN_1|\sigma|aN_2\rangle\langle aN_2| \\
& + \Gamma_{\downarrow} \sum_{N_1, N_2} |aN_1\rangle\langle bN_1|\sigma|bN_2\rangle\langle aN_2| \\
& - \Gamma_{\varphi} \sum_{N_1, N_2} |aN_1\rangle\langle aN_1|\sigma|bN_2\rangle\langle bN_2| \\
& - \Gamma_{\varphi} \sum_{N_1, N_2} |bN_1\rangle\langle bN_1|\sigma|aN_2\rangle\langle aN_2| \quad (24)
\end{aligned}$$

Below we assume that the interaction between the TLS and laser field does not influence the  $\Gamma$ 's rates and the corresponding rate equations. As was shown in<sup>23,24</sup>, this assumption is valid for relative weak driving, sufficient short correlation time of the heat bath  $\tau_c$ , and in large temperature limit:  $F \ll \Delta_{\varepsilon}, \hbar/\tau_c, k_B T$ <sup>25</sup>.

#### IV. BLOCH TYPE EQUATIONS FOR THE REDUCED DENSITY MATRIX

Equation (23) can be generalized to include the interaction between the TLS and laser field:

$$\frac{d\sigma}{dt} = -\frac{i}{\hbar}[H, \sigma] + \widehat{L} \quad (25)$$

where the Hamiltonian  $H$  is given in (3) with  $H_{int}$  in (4).

Following on, we define the reduced density matrix for the two level coupled system by tracing over the photon number  $N$ :

$$\begin{aligned}
\rho_{11} &= \sum_N \langle 1, N | \sigma | 1, N \rangle \\
\rho_{22} &= \sum_N \langle 2, N | \sigma | 2, N \rangle \\
\rho_{12} &= \sum_N \langle 1, N | \sigma | 2, N \rangle \\
\rho_{21} &= \sum_N \langle 2, N | \sigma | 1, N \rangle \quad (26)
\end{aligned}$$

$$\begin{aligned}
\kappa_{11} &= \sum_N \langle 1, N | \sigma | 1, N-1 \rangle \\
\kappa_{22} &= \sum_N \langle 2, N | \sigma | 2, N-1 \rangle \\
\kappa_{12} &= \sum_N \langle 1, N | \sigma | 2, N-1 \rangle \\
\kappa_{21} &= \sum_N \langle 2, N | \sigma | 1, N-1 \rangle \quad (27)
\end{aligned}$$

It is convenient to write the rate equations in terms of the new variables:  $\rho = \rho_{11} - \rho_{22}$ ,  $\rho_+ = \rho_{12} + \rho_{21}$ ,  $\rho_- = \rho_{12} - \rho_{21}$ ,  $\kappa^+ = \kappa_{11} + \kappa_{22}$ ,  $\kappa = \kappa_{11} - \kappa_{22}$ ,  $\kappa_+ = \kappa_{12} + \kappa_{21}$ ,  $\kappa_- = \kappa_{12} - \kappa_{21}$ . It is not difficult to show that the total population  $\rho^+ = \rho_{11} + \rho_{22}$  is constant:  $\frac{d\rho^+}{dt} = 0$  with the normalization condition  $\rho^+ = 1$ .

By taking into account the matrix elements of  $\widehat{L}$  in the dressed state basis (see Appendix A), we obtain the rate equations for the elements of the reduced density matrix:

$$\frac{d\rho}{dt} = -A_1\rho + B\rho_+ + \Gamma_- \cos 2\theta \quad (28)$$

$$\frac{d\rho_+}{dt} = -i\Omega_R\rho_- + B\rho - A_2\rho_+ + \Gamma_- \sin 2\theta \quad (29)$$

$$\frac{d\rho_-}{dt} = -i\Omega_R\rho_+ - \Gamma_{\varphi}\rho_- \quad (30)$$

$$\frac{d\kappa^+}{dt} = -i\omega_0\kappa^+ \quad (31)$$

$$\frac{d\kappa}{dt} = -i\omega_0\kappa - A_1\kappa + B\kappa_+ + \kappa^+\Gamma_- \cos 2\theta \quad (32)$$

$$\frac{d\kappa_+}{dt} = -i\omega_0\kappa_+ - i\Omega_R\kappa_- + B\kappa - A_2\kappa_+ + \kappa^+\Gamma_- \sin 2\theta \quad (33)$$

$$\frac{d\kappa_-}{dt} = -i\omega_0\kappa_- - i\Omega_R\kappa_+ - \Gamma_{\varphi}\kappa_- \quad (34)$$

where

$$A_1 = \left[ \frac{1}{T_1} \cos^2 2\theta + \Gamma_{\varphi} \sin^2 2\theta \right] \quad (35)$$

$$A_2 = \left[ \frac{1}{T_1} \sin^2 2\theta + \Gamma_{\varphi} \cos^2 2\theta \right] \quad (36)$$

$$B = \left[ \Gamma_{\varphi} - \frac{1}{T_1} \right] \sin 2\theta \cos 2\theta \quad (37)$$

The  $\rho$ 's elements of the density matrix describe the transitions between the Rabi levels, which are usually accounted for by a so called rotating wave approximation (RWA). The  $\kappa$ 's elements describe the transitions between neighboring manifolds spaced apart by the energy  $\hbar\omega_0$ . In the above equations it can be seen that these two types of transitions are completely independent: the equations for the  $\rho$  matrix are uncoupled from those for the  $\kappa$  matrix.

If the damping is absent (all  $\Gamma$ 's in (28), (29), (30) are equal to zero) the quantity  $\rho$  is constant, and  $\rho_+$  and  $\rho_-$  oscillate with the Rabi frequency  $\Omega_R$ . However, in the presence of damping these oscillations rapidly decay to their steady state values. Here it is instructive to consider two limiting cases.

### A. Bloch equations in the absence of a high frequency excitation

Let the power of high frequency photon field tends to zero. In this case  $\Omega_1 \rightarrow 0$ ,  $\omega_0 \rightarrow 0$ , and therefore,  $\sin 2\theta \rightarrow 0$ ,  $\cos 2\theta \rightarrow -1$ , and  $\Omega_R \rightarrow \Delta_\varepsilon/\hbar$ . From Eqs. (28), (29), (30) we get:

$$\frac{d\rho}{dt} = -\rho\frac{1}{T_1} - \Gamma_- \quad (38)$$

$$\frac{d\rho_+}{dt} = -i\frac{\Delta_\varepsilon}{\hbar}\rho_- - \Gamma_\varphi\rho_+ \quad (39)$$

$$\frac{d\rho_-}{dt} = -i\frac{\Delta_\varepsilon}{\hbar}\rho_+ - \Gamma_\varphi\rho_- \quad (40)$$

This result is obvious: the ladder of manifolds is reduced to just two levels  $|a\rangle$  and  $|b\rangle$ . The diagonal part of the density matrix relaxes with a rate of  $1/T_1$  to its steady state value  $\rho^{(0)} = -T_1\Gamma_-$ , while the offdiagonal elements  $\rho_\pm$  exhibit the damped oscillations with a rate  $\Gamma_\varphi$  and frequency  $\Delta_\varepsilon/\hbar$ .

### B. Bloch equations for zero high frequency detuning $\delta$ .

Consider the case when the high frequency detuning is zero ( $\delta = 0$ ). In this limit  $\sin 2\theta \rightarrow 1$ ,  $\cos 2\theta \rightarrow 0$  and we get from the Eqs. (28), (29), (30):

$$\frac{d\rho}{dt} = -\Gamma_\varphi\rho \quad (41)$$

$$\frac{d\rho_+}{dt} = -i\Omega_1\rho_- - \frac{1}{T_1}\rho_+ + \Gamma_- \quad (42)$$

$$\frac{d\rho_-}{dt} = -i\Omega_1\rho_+ - \Gamma_\varphi\rho_- \quad (43)$$

It is seen that the high frequency excitation drastically changes the behavior of the density matrix. Here the population  $\rho$  decays with the decoherence rate  $\Gamma_\varphi$ . This is due to the fact that the population of the level, say,  $|1, N\rangle$  can only be changed as a result of spontaneous transitions to the levels  $|1, N-1\rangle$  and  $|2, N-1\rangle$  of the neighboring manifold. The offdiagonal quantities  $\rho_+$  and  $\rho_-$  undergo the damped oscillations with a rate  $\frac{1}{2}\left(\frac{1}{T_1} + \Gamma_\varphi\right)$  provided that  $\Omega_1 > \frac{1}{2}\left(\frac{1}{T_1} - \Gamma_\varphi\right)$ .

### C. Steady state solution for the density matrix

The steady state solution ( $\frac{d\rho}{dt} = \frac{d\rho_-}{dt} = \frac{d\rho_+}{dt} = 0$ ) for Eqs. (28), (29), (30) is as follows:

$$\rho^{(0)} = \frac{(\Gamma_\varphi^2 + \Omega_R^2)}{\frac{\Gamma_\varphi^2}{T_1} + A_1\Omega_R^2}\Gamma_- \cos 2\theta \quad (44)$$

$$\rho_+^{(0)} = \frac{\Gamma_\varphi^2}{\frac{\Gamma_\varphi^2}{T_1} + A_1\Omega_R^2}\Gamma_- \sin 2\theta \quad (45)$$

$$\rho_-^{(0)} = -i\frac{\Omega_R}{\Gamma_\varphi}\rho_+^{(0)} \quad (46)$$

It is interesting to note that under high frequency irradiation the population of the Rabi levels becomes inverted. In (44), the quantity  $\rho^{(0)}$ , which is the difference of the populations between higher and lower Rabi levels, becomes positive, since for  $\delta > 0$  we have  $\cos 2\theta = -\delta/\Omega_R < 0$ , and always  $\Gamma_- < 0$ .

For the case when the high frequency detuning  $\delta$  is small compared to the Rabi frequency, at zero detuning ( $\delta \ll \Omega_1$ ), we have  $\sin 2\theta \rightarrow 1$  and  $\cos 2\theta \rightarrow -\delta/\Omega_1$ , and we get from Eqs. (44), (45), and (46):

$$\rho^{(0)} = -\frac{\delta}{\Gamma_\varphi\Omega_1} \frac{\Gamma_- (\Gamma_\varphi^2 + \Omega_1^2)}{\Omega_1^2 + \frac{\Gamma_\varphi^2}{T_1}} \quad (47)$$

$$\rho_+^{(0)} = \frac{\Gamma_- \Gamma_\varphi}{\Omega_1^2 + \frac{\Gamma_\varphi^2}{T_1}} \quad (48)$$

$$\rho_-^{(0)} = -i\frac{\Gamma_- \Omega_1}{\Omega_1^2 + \frac{\Gamma_\varphi^2}{T_1}} \quad (49)$$

As seen from (47)  $\rho^{(0)} \rightarrow 0$  as  $\delta$  tends to zero. This causes the equalization of the population of the two levels ( $\rho_{11} = \rho_{22} = \frac{1}{2}$ ) when the high frequency is in exact resonance with the energy gap of the TLS.

The steady state solutions of Eqs. (31), (32), (33), and (34) are equal to zero:  $\kappa^+(0) = 0$ ,  $\kappa^-(0) = 0$ ,  $\kappa_+^{(0)} = 0$ ,  $\kappa_-^{(0)} = 0$ . This implies  $\kappa_{11}^{(0)} = 0$ ,  $\kappa_{22}^{(0)} = 0$ ,  $\kappa_{12}^{(0)} = 0$ , and  $\kappa_{21}^{(0)} = 0$ .

### V. EXCITATION OF RABI LEVELS BY A LOW FREQUENCY SIGNAL

In this section we find the response of the TLS coupled to a photon field to an external signal the frequency of which is of the order of the Rabi frequency  $\Omega_R$ . The

operator equation for the density matrix  $\sigma$  is similar to (25):

$$\frac{d\sigma}{dt} = -\frac{i}{\hbar}[H + H_{int}^{LF}, \sigma] + \hat{L} \quad (50)$$

where the Hamiltonian  $H_{int}^{LF}$  is given in (15).

Since the low frequency signal cannot change the photon number  $N$ , the transitions between Rabi levels  $|1, N\rangle$  and  $|2, N\rangle$  can be induced only by the second term in the low frequency Hamiltonian (15). The equations for the  $\rho$ 's and the  $\kappa$ 's are obtained in the same way as used for Eqs. (28)- (34). The only difference is the appearance of low frequency terms in the right hand side of these equations. Therefore, by taking into account the low frequency excitation, we get the following Bloch like equations for the reduced density matrix:

$$\begin{aligned} \frac{d\rho}{dt} = & -A_1\rho + B\rho_+ - \rho_- (ig_1 \sin 2\theta \cos \omega t) + \\ & - ig_2 \cos \omega t \cos^2 \theta (\kappa_{12} - \kappa_{12}^+) + \Gamma_- \cos 2\theta \end{aligned} \quad (51)$$

$$\frac{d\rho^+}{dt} = -ig_2 \cos \omega t \sin^2 \theta (\kappa_{21} - \kappa_{21}^+) \quad (52)$$

$$\begin{aligned} \frac{d\rho_+}{dt} = & -i\Omega_R\rho_- + B\rho - A_2\rho_+ + \rho_- (ig_1 \cos 2\theta \cos \omega t) \\ & + ig_2 \cos \omega t [(\kappa_{22}^+ - \kappa_{22}) + (\kappa_{11}^+ - \kappa_{11}) \cos 2\theta + \\ & (\kappa_{21} + \kappa_{12}^+ - \kappa_{21}^+ - \kappa_{12}) \sin 2\theta] + \Gamma_- \sin 2\theta \end{aligned} \quad (53)$$

$$\begin{aligned} \frac{d\rho_-}{dt} = & -i\Omega_R\rho_+ - \Gamma_\varphi\rho_- + ig_1 (\rho_+ \cos 2\theta - \rho \sin 2\theta) \cos \omega t \\ & - ig_2 \cos \omega t [\sin 2\theta (\kappa_{12} + \kappa_{12}^+ + \kappa_{21} + \kappa_{21}^+) \\ & - (\kappa_{11} + \kappa_{11}^+) - (\kappa_{22} + \kappa_{22}^+) \cos 2\theta] \end{aligned} \quad (54)$$

where  $g_1 = 2\varepsilon G/\hbar\Delta_\varepsilon$ , and  $g_2 = 2\Delta G/\hbar\Delta_\varepsilon$ .

$$\begin{aligned} \frac{d\kappa}{dt} = & -i\omega_0\kappa - A_1\kappa + B\kappa_+ + \kappa^+\Gamma_- \cos 2\theta \\ & + ig_2 \cos \omega t [\rho_+ - \rho_- \cos 2\theta] - ig_1\kappa_- \cos \omega t \sin 2\theta \end{aligned} \quad (55)$$

$$\begin{aligned} \frac{d\kappa_+}{dt} = & -i\omega_0\kappa_+ - i\Omega_R\kappa_- + B\kappa - A_2\kappa_+ + \kappa^+\Gamma_- \sin 2\theta \\ & - ig_2 \cos \omega t [\rho_- \sin 2\theta + \rho] + ig_1\kappa_- \cos \omega t \cos 2\theta \end{aligned} \quad (56)$$

$$\begin{aligned} \frac{d\kappa_-}{dt} = & -i\omega_0\kappa_- - i\Omega_R\kappa_+ - \Gamma_\varphi\kappa_- \\ & - ig_2 \cos \omega t [\rho_+ \sin 2\theta + \rho \cos 2\theta] \\ & + ig_1 \cos \omega t [\kappa_+ \cos 2\theta - \kappa \sin 2\theta] \end{aligned} \quad (57)$$

The equation for  $\kappa^+$  remains unchanged (Eq. (31)). Therefore, the low frequency excitation couples the  $\rho$  and  $\kappa$  elements of the reduced density matrix. Due to this coupling the  $\kappa$  elements acquire the low frequency part which thus should be included in the standard scheme of RWA.

## VI. LOW FREQUENCY LINEAR SUSCEPTIBILITIES FOR THE TLS

It is evident that the above equations exhibit oscillatory solutions in the presence of damping. For a small amplitude low frequency signal,  $G$  the time dependent solution for Eqs. (51), (52), (53), and (54) can be obtained by using a perturbation method where the small time-dependent corrections to the steady state values are:  $\rho(t) = \rho^{(0)} + \rho^{(1)}(t)$ ,  $\rho_+(t) = \rho_+^{(0)} + \rho_+^{(1)}(t)$ , and  $\rho_-(t) = \rho_-^{(0)} + \rho_-^{(1)}(t)$ . By doing this we may neglect all  $\kappa$ 's on the right hand side of these equations, since the steady state values for the  $\kappa$ 's are zero. Therefore, in this approximation the equations for the time dependent corrections to the  $\rho$ 's are decoupled from those to the  $\kappa$ 's:

$$\frac{d\rho^{(1)}}{dt} = -A_1\rho^{(1)} + B\rho_+^{(1)} - \rho_-^{(0)} (ig \sin 2\theta \cos \omega t) \quad (58)$$

$$\frac{d\rho_+^{(1)}}{dt} = -i\Omega_R\rho_-^{(1)} + B\rho^{(1)} - A_2\rho_+^{(1)} + \rho_-^{(0)} (ig \cos 2\theta \cos \omega t) \quad (59)$$

$$\begin{aligned} \frac{d\rho_-^{(1)}}{dt} = & -i\Omega_R\rho_+^{(1)} - \Gamma_\varphi\rho_-^{(1)} + \\ & ig \left( \rho_+^{(0)} \cos 2\theta - \rho^{(0)} \sin 2\theta \right) \cos \omega t \end{aligned} \quad (60)$$

where  $\rho^{(0)}$ ,  $\rho_+^{(0)}$ , and  $\rho_-^{(0)}$  are the steady state values given in (44), (45), and (46).

From these equations it is not difficult to find the linear susceptibilities of the system ( $\chi_\rho(\omega) = \rho(\omega)/G(\omega)$ , etc.):

$$\chi_\rho(\omega) = -\frac{2\varepsilon\Omega_R}{D(\omega)\hbar\Gamma_\varphi\Delta_\varepsilon}\rho_+^{(0)} \left[ \sin 2\theta \left[ (i\omega + \Gamma_\varphi) \left( i\omega + \frac{1}{T_1} \right) + \Omega_R^2 \right] + \frac{\Omega_R^2}{\Gamma_\varphi} B \cos 2\theta \right] \quad (61)$$

$$\chi_{\rho_+}(\omega) = \frac{2\varepsilon\Omega_R}{D(\omega)\hbar\Gamma_\varphi\Delta_\varepsilon} \cos 2\theta \rho_+^{(0)} \left[ (i\omega + \Gamma_\varphi) \left( i\omega + \frac{1}{T_1} \right) - (i\omega + A_1) \frac{\Omega_R^2}{\Gamma_\varphi} \right] \quad (62)$$

$$\chi_{\rho_-}(\omega) = -i \frac{2\varepsilon\Omega_R^2}{D(\omega)\hbar\Gamma_\varphi^2\Delta_\varepsilon} \rho_+^{(0)} \cos 2\theta \left( i\omega + \frac{1}{T_1} \right) (i\omega + 2\Gamma_\varphi) \quad (63)$$

where

$$D(\omega) = (i\omega + \Gamma_\varphi)^2 \left( i\omega + \frac{1}{T_1} \right) + (i\omega + A_1) \Omega_R^2 \quad (64)$$

Eqs. (61), (62), and (63) give the response of the coupled system (TLS and associated photon field) to a low frequency signal, which excites transitions between the Rabi levels.

From (61), (62), and (63) the linear susceptibilities for the case of small high frequency detuning,  $\sin 2\theta \rightarrow 1$ ,  $\cos 2\theta \rightarrow -\delta/\Omega_1$ ,  $A_1 \rightarrow \Gamma_\varphi$ ,  $A_2 \rightarrow 1/T_1$ , and  $B \rightarrow -\frac{\delta}{\Omega_1} \left( \Gamma_\varphi - \frac{1}{T_1} \right)$ , can also be obtained.

$$\chi_\rho(\omega) = -\frac{2\varepsilon\Omega_1}{\hbar\Delta_\varepsilon\Gamma_\varphi} \frac{\rho_+^{(0)}}{i\omega + \Gamma_\varphi} \quad (65)$$

$$\chi_{\rho_+}(\omega) = -\delta \frac{2\varepsilon}{\hbar\Delta_\varepsilon} \frac{\rho_+^{(0)}}{\Gamma_\varphi d(\omega)} \left[ i\omega + \frac{1}{T_1} - \frac{\Omega_1^2}{\Gamma_\varphi} \right] \quad (66)$$

$$\chi_{\rho_-}(\omega) = i\delta \frac{2\varepsilon}{\hbar\Delta_\varepsilon} \frac{\Omega_1 \rho_+^{(0)}}{\Gamma_\varphi^2 d(\omega)} \frac{\left( i\omega + \frac{1}{T_1} \right) (i\omega + 2\Gamma_\varphi)}{(i\omega + \Gamma_\varphi)} \quad (67)$$

where

$$d(\omega) = \left( i\omega + \frac{1}{T_1} \right) (i\omega + \Gamma_\varphi) + \Omega_1^2 \quad (68)$$

and  $\rho_+^{(0)}$  is given by (48). The resonance nature of the response is evident from (68).

The equations for the time dependent  $\kappa$ 's in the first order in  $g$  are coupled to  $\rho$ 's via their steady state values

as follows:

$$\frac{d\kappa^+}{dt} = -i\omega_0\kappa^+ \quad (69)$$

$$\begin{aligned} \frac{d\kappa}{dt} = & -i\omega_0\kappa - A_1\kappa + B\kappa_+ + \kappa^+\Gamma_- \cos 2\theta \\ & + i\frac{g_2}{2}f_1 \cos \omega t \end{aligned} \quad (70)$$

$$\begin{aligned} \frac{d\kappa_+}{dt} = & -i\omega_0\kappa_+ - i\Omega_R\kappa_- + B\kappa - A_2\kappa_+ + \kappa^+\Gamma_- \sin 2\theta \\ & - i\frac{g_2}{2}f_2 \cos \omega t \end{aligned} \quad (71)$$

$$\frac{d\kappa_-}{dt} = -i\omega_0\kappa_- - i\Omega_R\kappa_+ - \Gamma_\varphi\kappa_- - i\frac{g_2}{2}f_3 \cos \omega t \quad (72)$$

where

$$f_1 = \left( \rho_+^{(0)} - \rho_-^{(0)} \cos 2\theta \right) \quad (73)$$

$$f_2 = \left( \rho_-^{(0)} \sin 2\theta + \rho^{(0)} \right) \quad (74)$$

$$f_3 = \left( \rho_+^{(0)} \sin 2\theta + \rho^{(0)} \cos 2\theta \right) \quad (75)$$

---

The low frequency linear susceptibilities for the  $\kappa$ 's ( $\chi_\kappa(\omega) = \kappa(\omega)/G(\omega)$ , etc.) are as follows:  $\chi_{\kappa^+}(\omega) = 0$ ,

$$\chi_{\kappa_-}(\omega) = \frac{\Delta}{\hbar\Delta_\varepsilon D_0(\omega)} \left( -if_3 [i(\omega + \omega_0) + A_1] [i(\omega + \omega_0) + A_2] + f_1 B \Omega_R + if_3 B^2 - f_2 \Omega_R [i(\omega + \omega_0) + A_1] \right) \quad (76)$$

$$\chi_\kappa(\omega) = \frac{\Delta}{\hbar\Delta_\varepsilon D_0(\omega)} \left( if_1 [i(\omega + \omega_0) + A_2] [i(\omega + \omega_0) + \Gamma_\varphi] - if_2 B [i(\omega + \omega_0) + \Gamma_\varphi] - f_3 B \Omega_R + if_3 \Omega_R^2 \right) \quad (77)$$

$$\chi_{\kappa_+}(\omega) = \frac{\Delta}{\hbar\Delta_\varepsilon D_0(\omega)} \left( -if_2 [i(\omega + \omega_0) + A_1] [i(\omega + \omega_0) + \Gamma_\varphi] + if_1 B [i(\omega + \omega_0) + \Gamma_\varphi] - f_3 \Omega_R [i(\omega + \omega_0) + A_1] \right) \quad (78)$$

where

$$D_0(\omega) = [i(\omega + \omega_0) + \Gamma_\varphi]^2 \left( i(\omega + \omega_0) + \frac{1}{T_1} \right) + [i(\omega + \omega_0) + A_1] \Omega_R^2 \quad (79)$$

By assuming that the gap frequency  $\omega_0$  is much more than  $\omega$  and the rates  $\Gamma$ 's, we obtain from (76), (77), and (78) the corresponding low frequency susceptibilities in the second order of the inverse frequency  $\omega_0$ :

$$\chi_{\kappa_-}(\omega) = -\frac{\Delta}{\hbar\omega_0\Delta_\varepsilon} f_3 + \frac{\Delta}{\hbar\omega_0^2\Delta_\varepsilon} (-i\Gamma_\varphi f_3 + \omega f_3 + f_2\Omega_R) \quad (80)$$

$$\chi_\kappa(\omega) = \frac{\Delta}{\hbar\omega_0\Delta_\varepsilon} f_1 + i\frac{\Delta}{\hbar\omega_0^2\Delta_\varepsilon} (A_1 f_1 + f_2 B) \quad (81)$$

$$\begin{aligned} \chi_{\kappa_+}(\omega) = & -\frac{\Delta}{\hbar\omega_0\Delta_\varepsilon} f_2 \\ & + \frac{\Delta}{\hbar\omega_0^2\Delta_\varepsilon} (-iA_2 f_2 + \omega f_2 + f_3\Omega_R - i f_1 B) \end{aligned} \quad (82)$$

## VII. THE APPLICATIONS

In possible applications of the method that we propose here the quantities to be measured are the averages of the Pauli spin operators  $\langle\sigma_X\rangle$ ,  $\langle\sigma_Y\rangle$ ,  $\langle\sigma_Z\rangle$ , and their time derivatives  $\frac{d\langle\sigma_X\rangle}{dt}$ ,  $\frac{d\langle\sigma_Y\rangle}{dt}$ ,  $\frac{d\langle\sigma_Z\rangle}{dt}$ . By using the definitions of the density matrix (26) and (27), and the dressed states (9) and (10) we obtain from the direct application of Eqs. (115) and (116) (see Appendix B):

$$\langle\sigma_Z\rangle = \rho(t) \cos 2\theta + \rho_+(t) \sin 2\theta \quad (83)$$

$$\langle\sigma_X\rangle = \sin 2\theta \text{Re}[\kappa(t)] - \cos 2\theta \text{Re}[\kappa_+(t)] - \text{Re}[\kappa_-(t)] \quad (84)$$

$$\langle\sigma_Y\rangle = -\sin 2\theta \text{Im}[\kappa(t)] + \cos 2\theta \text{Im}[\kappa_+(t)] + \text{Im}[\kappa_-(t)] \quad (85)$$

For a small amplitude low frequency excitation  $G \cos \omega t$  we calculate, below, the time derivatives of (83), (84), and (85) with the help of equations (58), (59), and (60) for the  $\rho$ 's and (70), (71), and (72) for the  $\kappa$ 's:

$$\begin{aligned} \frac{d\langle\sigma_X\rangle}{dt} = & \omega_0 \sin 2\theta \text{Im}[\kappa(t)] - \Gamma_\varphi \sin 2\theta \text{Re}[\kappa(t)] \\ & + \Gamma_\varphi \cos 2\theta \text{Re}[\kappa_+(t)] - (\omega_0 + \Omega_R \cos 2\theta) \text{Im}[\kappa_-(t)] \\ & - (\omega_0 \cos 2\theta + \Omega_R) \text{Im}[\kappa_+(t)] + \Gamma_\varphi \text{Re}[\kappa_-(t)] \end{aligned} \quad (86)$$

$$\begin{aligned} \frac{d\langle\sigma_Y\rangle}{dt} = & \omega_0 \sin 2\theta \text{Re}[\kappa(t)] + \Gamma_\varphi \sin 2\theta \text{Im}[\kappa(t)] \\ & - \Gamma_\varphi \cos 2\theta \text{Im}[\kappa_+(t)] - (\omega_0 + \Omega_R \cos 2\theta) \text{Re}[\kappa_-(t)] \\ & - (\omega_0 \cos 2\theta + \Omega_R) \text{Re}[\kappa_+(t)] - \Gamma_\varphi \text{Im}[\kappa_-(t)] - g_2 f_3 \cos \omega t \end{aligned} \quad (87)$$

$$\frac{d\langle\sigma_Z\rangle}{dt} = -\frac{1}{T_1} \langle\sigma_Z\rangle - i\Omega_R \sin 2\theta \rho_-^{(0)} - i\Omega_R \sin 2\theta \rho_-^{(1)}(t) + \Gamma_- \quad (88)$$

where  $\langle\sigma_Z\rangle$  in the right hand side of (88) is written using the first approximation only:

$$\langle\sigma_Z\rangle = \rho^{(0)} \cos 2\theta + \rho_+^{(0)} \sin 2\theta + \rho^{(1)}(t) \cos 2\theta + \rho_+^{(1)}(t) \sin 2\theta \quad (89)$$

The quantities  $\rho^{(1)}(t)$ ,  $\rho_+^{(1)}(t)$ , and  $\rho_-^{(1)}(t)$  can be expressed in terms of the real ( $\chi'$ ) and imaginary ( $\chi''$ ) parts of their corresponding low frequency susceptibilities:  $\rho^{(1)}(t) = G(\chi'_\rho \cos \omega t - \chi''_\rho \sin \omega t)$ ,  $\rho_+^{(1)}(t) = G(\chi'_{\rho_+} \cos \omega t - \chi''_{\rho_+} \sin \omega t)$ , and  $\rho_-^{(1)}(t) = iG(\chi'_{\rho_-} \sin \omega t + \chi''_{\rho_-} \cos \omega t)$ .

### A. Flux qubit

Our method can be directly applied to a persistent current qubit (flux qubit), which is a superconducting loop interrupted by three Josephson junctions<sup>28,29</sup>. For these qubits the successful experimental implementation of the low frequency readout electronics has been demonstrated<sup>13,30,31</sup>. Though the main subject of the paper is the combined effect on the TLS of the high and low frequencies, it is worth noting that the pure low frequency probing of the TLS can also be a valuable tool for characterization of the two-level systems. In fact, for the flux qubit this method has been realized theoretically and experimentally<sup>30,31</sup>.

The basis qubit states have opposing persistent currents. The operator of the persistent current in the qubit loop is  $\hat{I}_q = I_q \sigma_z$ . In eigenstate basis the average current,  $\langle\hat{I}_q\rangle$  is:

$$\langle\hat{I}_q\rangle = \frac{I_q}{\Delta_\varepsilon} (\varepsilon \langle\sigma_Z\rangle - \Delta \langle\sigma_X\rangle). \quad (90)$$

This current can be detected by a high quality resonant tank circuit inductively coupled to the qubit loop<sup>13,30,31</sup> (see Fig. 3). For the flux qubit the bias  $\varepsilon$  is controlled by an external dc flux  $\Phi_X$ :  $\varepsilon = E_J(\Phi_X/\Phi_0 - 1/2)$ ,

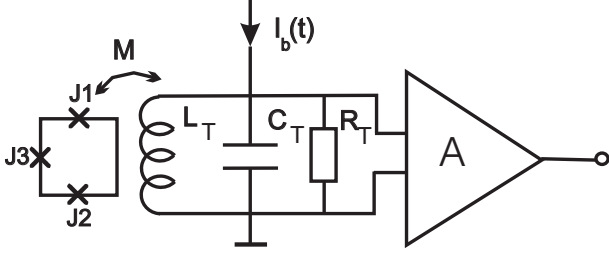


FIG. 3: Flux qubit coupled to a high quality resonant tank circuit.

where  $E_J = \Phi_0 I_q / 2\pi$ , and  $\Phi_0 = h/2e$  is the flux quantum. The qubit is inductively coupled through the mutual inductance  $M = k(L_q L_T)^{1/2}$ , where  $k$  is the dimensionless coupling parameter, and  $L_q$  is the inductance of the qubit loop, to a high quality resonant tank circuit with inductance  $L_T$ , capacitance  $C_T$ , and quality factor

$Q_T$ . The tank circuit is biased by a low (compared to the gap) frequency current  $I_b = I_0 \cos \omega t$ . In addition, a high frequency signal  $F \cos \omega_0 t$  (not shown in Fig. 3) tuned to the gap frequency  $\Delta_\varepsilon / \hbar$  is applied to the qubit loop. This readout circuit has prove to be successful for the investigation of the quantum properties of the flux qubit<sup>13,30,31</sup>. The interaction between the qubit and the tank circuit is described by the term  $G(t) = M I_q I_T(t)$ , where  $I_q$  is the current flowing in the qubit loop, and  $I_T$  is the current in the tank coil. The voltage across the tank,  $V(t) = V_T \cos(\omega t + \chi)$ , is given by<sup>30</sup>:

$$\ddot{V} + \gamma_T \dot{V} + \omega_T^2 V = -M \omega_T^2 \frac{d\langle \hat{I}_q \rangle}{dt} + \omega_T^2 L_T \dot{I}_b, \quad (91)$$

where  $\gamma_T = \omega_T / Q_T$ , and  $\omega_T = (L_T C_T)^{-1/2}$  is the tank resonance frequency, which is tuned to the Rabi frequency ( $\omega_T \simeq \Omega_R$ ). By using (86) and (88) we find:

$$\begin{aligned} \frac{d\langle \hat{I}_q \rangle}{dt} = & -\frac{I_q \varepsilon}{\Delta_\varepsilon T_1} [\rho(t) \cos 2\theta + \rho_+(t) \sin 2\theta + i\Omega_R T_1 \sin 2\theta \rho_-(t)] - \frac{I_q \Delta}{\Delta_\varepsilon} \{ \omega_0 \sin 2\theta \text{Im}[\kappa(t)] - \Gamma_\varphi \sin 2\theta \text{Re}[\kappa(t)] + \Gamma_\varphi \text{Re}[\kappa_-(t)] \\ & + \Gamma_\varphi \cos 2\theta \text{Re}[\kappa_+(t)] - (\omega_0 + \Omega_R \cos 2\theta) \text{Im}[\kappa_-(t)] - (\omega_0 \cos 2\theta + \Omega_R) \text{Im}[\kappa_+(t)] \} \end{aligned} \quad (92)$$

In order to write down the Fourier component of (92) we use the relations  $(\text{Im}[k(t)])_\omega = \frac{1}{2i} (\chi_\kappa(\omega) - \chi_\kappa^*(-\omega)) G(\omega)$ ,  $(\text{Re}[k(t)])_\omega = \frac{1}{2} (\chi_\kappa(\omega) + \chi_\kappa^*(-\omega)) G(\omega)$ , etc... Therefore,

$$\begin{aligned} \left( \frac{d\langle \hat{I}_q \rangle}{dt} \right)_\omega = & -\frac{I_q \varepsilon G(\omega)}{\Delta_\varepsilon T_1} [\chi_\rho(\omega) \cos 2\theta + \chi_{\rho_+}(\omega) \sin 2\theta + i\Omega_R T_1 \sin 2\theta \chi_{\rho_-}(\omega)] - \frac{I_q \Delta G(\omega)}{2\Delta_\varepsilon} \{ -i\omega_0 \sin 2\theta [\chi_\kappa(\omega) - \chi_\kappa^*(-\omega)] \\ & + \Gamma_\varphi [\chi_{\kappa_-}(\omega) + \chi_{\kappa_-}^*(-\omega)] - \Gamma_\varphi \sin 2\theta [\chi_\kappa(\omega) + \chi_\kappa^*(-\omega)] + \Gamma_\varphi \cos 2\theta [\chi_{\kappa_+}(\omega) + \chi_{\kappa_+}^*(-\omega)] \\ & + i(\omega_0 + \Omega_R \cos 2\theta) [\chi_{\kappa_-}(\omega) - \chi_{\kappa_-}^*(-\omega)] + i(\omega_0 \cos 2\theta + \Omega_R) [\chi_{\kappa_+}(\omega) - \chi_{\kappa_+}^*(-\omega)] \} \end{aligned} \quad (93)$$

where the expressions for the susceptibilities are given in (61), (62), (63), (76), (77), and (78). Eq. (91) in terms of its Fourier components reads:

$$V(\omega) (\omega_T^2 - \omega^2 + i\omega\gamma_T) = -M \omega_T^2 \left( \frac{d\langle \hat{I}_q \rangle}{dt} \right)_\omega + i\omega \omega_T^2 L_T I_0 \quad (94)$$

By taking into account that  $G(\omega) = M I_q I_T(\omega)$ , where  $I_T(\omega) = -iV(\omega)/\omega L_T$ , we obtain for the low frequency detuning  $\xi$ , and friction,  $\Gamma_T$ :

$$\begin{aligned} \xi = & \omega_T^2 - \omega^2 - \frac{k^2 \omega_T L_q I_q^2 \varepsilon}{\Delta_\varepsilon T_1} \left( \Omega_R T_1 \sin 2\theta \chi'_{\rho_-}(\omega) + \cos 2\theta \chi''_{\rho}(\omega) + \sin 2\theta \chi''_{\rho_+}(\omega) \right) \\ & - \frac{k^2 \omega_T L_q I_q^2 \Delta}{2\Delta_\varepsilon} \left( -\omega_0 \sin 2\theta [\chi'_\kappa(\omega) - \chi'_\kappa(-\omega)] + \Gamma_\varphi [\chi''_{\kappa_-}(\omega) - \chi''_{\kappa_-}(-\omega)] - \Gamma_\varphi \sin 2\theta [\chi''_\kappa(\omega) - \chi''_\kappa(-\omega)] \right. \\ & \left. + \Gamma_\varphi \cos 2\theta [\chi''_{\kappa_+}(\omega) - \chi''_{\kappa_+}(-\omega)] + (\omega_0 \cos 2\theta + \Omega_R) [\chi'_{\kappa_+}(\omega) - \chi'_{\kappa_+}(-\omega)] + (\omega_0 + \Omega_R \cos 2\theta) [\chi'_{\kappa_-}(\omega) - \chi'_{\kappa_-}(-\omega)] \right) \end{aligned} \quad (95)$$

$$\begin{aligned}
\Gamma_T = & \gamma_T - \frac{k^2 L_q I_q^2 \varepsilon}{\Delta \varepsilon T_1} \left( \Omega_R T_1 \sin 2\theta \chi''_{\rho_-}(\omega) - \cos 2\theta \chi'_{\rho}(\omega) - \sin 2\theta \chi'_{\rho_+}(\omega) \right) \\
& + \frac{k^2 L_q I_q^2 \Delta}{2\Delta \varepsilon} \left( \omega_0 \sin 2\theta [\chi''_{\kappa}(\omega) + \chi''_{\kappa}(-\omega)] + \Gamma_{\varphi} [\chi'_{\kappa_-}(\omega) + \chi'_{\kappa_-}(-\omega)] - \Gamma_{\varphi} \sin 2\theta [\chi'_{\kappa}(\omega) + \chi'_{\kappa}(-\omega)] \right) \\
& + \Gamma_{\varphi} \cos 2\theta [\chi'_{\kappa_+}(\omega) + \chi'_{\kappa_+}(-\omega)] - (\omega_0 \cos 2\theta + \Omega_R) [\chi''_{\kappa_+}(\omega) + \chi''_{\kappa_+}(-\omega)] - (\omega_0 + \Omega_R \cos 2\theta) [\chi''_{\kappa_-}(\omega) + \chi''_{\kappa_-}(-\omega)] \quad (96)
\end{aligned}$$

From (95), and (96) we obtain the voltage amplitude  $V_T$ , and the phase,  $\chi$ :  $V_T = \omega \omega_T^2 L_T I_0 / \sqrt{\xi^2 + \omega^2 \Gamma_T^2}$ , and  $tg\chi = \xi / \omega \Gamma_T$ .

These expressions have two different parts. The terms which are proportional to  $\varepsilon$  are due to transitions between the Rabi levels. These terms have a resonance at the Rabi frequency and they vanish at the optimal point (at  $\varepsilon = 0$ ). Other, nonresonant, terms come from the transitions at the frequency  $\omega_0$  between neighboring manifolds. The contribution of these terms does not vanish at the optimal point.

By assuming that the gap frequency  $\omega_0$  is much more than  $\omega$  and the rates  $\Gamma$ 's, we obtain at  $\varepsilon = 0$  with the help of the susceptibilities (80), (81), and (82) the expressions for low frequency detuning  $\xi$  and friction  $\Gamma_T$ :

$$\begin{aligned}
\xi = & \omega_T^2 - \omega^2 - 2 \frac{k^2 L_q I_q^2 \omega_T^2}{\Delta} \tilde{\rho}_+^{(0)} \\
& \times \left[ 1 + \frac{\delta^2}{\Gamma_{\varphi}^2} - \frac{\delta}{\omega_0} \left( 1 + \frac{\Omega_1^2 + \delta^2}{2\Gamma_{\varphi}^2} \right) \right] \quad (97)
\end{aligned}$$

$$\begin{aligned}
\Gamma_T = & \gamma_T + \frac{k^2 L_q I_q^2}{\Delta} \left( \frac{\delta}{\omega_0} \right) \Gamma_{\varphi} \tilde{\rho}_+^{(0)} \\
& \times \left[ 3 + \frac{2\Omega_R^2}{\Gamma_{\varphi}^2} + \frac{\Omega_R^2}{T_1 \Gamma_{\varphi}^3} + \frac{\delta^2}{\Omega_R^2} \left( 1 + \frac{2\Omega_R^2}{\Gamma_{\varphi}^2} - \frac{\Omega_R^2}{T_1 \Gamma_{\varphi}^3} \right) \right] \quad (98)
\end{aligned}$$

where

$$\tilde{\rho}_+^{(0)} = \frac{\Gamma_{\varphi}^2 \Gamma - T_1}{\Gamma_{\varphi}^2 + A_1 \Omega_R^2 T_1} \quad (99)$$

At the point of resonance ( $\delta = 0$ ) the response of the flux qubit is purely inductive,  $\Gamma_T = \gamma_T$ . It is interesting to note that expression (98) predicts the "cooling down" of the irradiated qubit due to its interaction with the tank circuit. Since  $\Gamma - T_1$  is negative (see (22)) the quantity  $\Gamma_T$  at  $\delta > 0$  is less than  $\gamma_T$ , i. e. the quality factor of the tank is increased. The energy from the qubit transfers to the tank: the qubit is cooled, the tank is heated. The effect is more pronounced if ( $\delta \gg \Omega_1$ ). For this case expression (98) is reduced to:

$$\Gamma_T = \gamma_T - 4 \frac{k^2 L_q I_q^2}{\Delta} \left( \frac{\delta}{\omega_0} \right) \Gamma_{\varphi} \tanh \left( \frac{\Delta}{2k_B T} \right) \quad (100)$$

Similar effects have been observed in<sup>13</sup>. These experiments showed an increase in the quality of the tank resonator by approximately a factor of 2. For the estimation of  $\Gamma_T$  we take the parameters of the flux qubit used in<sup>13</sup>:  $\Delta/\hbar = 1$  GHz,  $L_q = 24$  pH,  $\omega_T/2\pi = 6.284$  MHz, the tank quality factor  $Q_T = 1850$ ,  $\gamma_T = \omega_T/Q_T = 2.0 \times 10^4$ ,  $I_q = 600$  nA,  $L_T = 0.2\mu\text{H}$ ,  $M = 70$  pH,  $\Gamma_{\varphi} = 8 \times 10^5 \text{c}^{-1}$ , and  $\Omega_1 \sim \omega_T$ . The result is  $\Gamma_T \approx \gamma_T - 2 \times 10^4 \left( \frac{\delta}{\omega_0} \right)$ . For  $\delta \approx 0.1\omega_0$  we obtain an increase in the quality factor of the tank by approximately 15%. Therefore, for the parameters we used expression (98) gives a relatively weak effect.

As was shown by Ju. Hauss et al. (2007)<sup>17</sup>, an additional contribution to the heating of the tank, which can explain the observed amplitude, appears in the second order terms in  $G$  (which is beyond our linear approximation) at twice the Rabi frequency  $\omega \approx 2\Omega_R$ . The effect appears at nonzero high frequency detuning  $\delta$  as a result of the "negative temperature" of the Rabi levels mentioned before in connection with Eq.(44).

## B. Nuclear magnetic resonance

Another application of the method can be made to nuclear magnetic resonance (NMR). The basic input scheme of any NMR device is similar to that shown in Fig. 3, where a sample with a substance under study replaces the flux qubit loop. The common mode of operation of the NMR device is to polarize the sample with a relatively high static magnetic field  $B_0$  and at the same time apply a time dependent magnetic field  $B_1 \cos \omega_0 t$  perpendicular to  $B_0$ . The amplitude of the excitation signal is rather low ( $B_1 \ll B_0$ ) and it is tuned to the NMR resonance frequency ( $\omega_0 \approx \gamma B_0$ ), where  $\gamma$  is the gyromagnetic ratio. The tank circuit detects the time derivatives (Faraday law of induction) of the transversal magnetizations  $M_X$  and  $M_Y$  which oscillate with the high NMR frequency  $\gamma B_0$ . In addition, under the excitation  $B_1 \cos \omega_0 t$  the longitudinal magnetization  $M_Z$  oscillates with the Rabi frequency  $\Omega_R \approx \gamma B_1$ , and sidebands  $\omega_0 \pm \Omega_R$  appear in the transversal components  $M_X$  and  $M_Y$ . However, due to coupling to the environment, which is described by the relaxation  $T_1$  and dephasing  $T_2$  times in Bloch equations, the Rabi oscillations undergo fast decay and disappear from the output signal. The application to the sample of another low frequency signal  $B_{LF} \cos \omega t$ , which

is tuned to the Rabi frequency ( $\omega \approx \Omega_R$ ) causes a persistent low frequency oscillation of the magnetization with its resonance at the Rabi frequency.

The case of NMR differs from the previous example in that here we deal with a real spin-1/2 particle. Therefore, all components  $\langle \sigma_i \rangle$  ( $i = X, Y, Z$ ) of the averaged spin operator and their time derivatives are accessible for the measurements. As distinct from the flux qubit case, where the low and high frequency excitations are coupled only to  $\sigma_z$  (see Eq. 2) in NMR we may couple the low frequency and high frequency fields separately to any component of the spin operator. In order to simplify the problem we consider the following Hamiltonian for the spin-1/2 particle in an external magnetic field:

$$H = \frac{\hbar\gamma B_0}{2}\sigma_Z + \frac{\hbar\gamma}{2}\sigma_Z B_{LF} \cos\omega t + \frac{\hbar\gamma}{2}\sigma_X B_1 \cos\omega_0 t \quad (101)$$

where we choose the  $z$  axis to be along the polarizing field  $B_0$ , and the sign in (101) is consistent with our convention  $\sigma_Z|a\rangle = -|a\rangle$ ,  $\sigma_Z|b\rangle = |b\rangle$ .

The high frequency excitation signal  $B_1 \cos\omega_0 t$ , which is tuned to the NMR resonance frequency  $\gamma B_0$ , is applied along the  $x$  axis, and a low frequency signal  $B_{LF} \cos\omega t$ , which is tuned to the Rabi frequency,  $\omega \approx \Omega_R$ , is applied along the  $z$  axis. It is just the low frequency component in (101) that causes the transitions between the Rabi levels.

Since the low frequency component is applied only along one axis (as distinct from (15)),  $g_2 = 0$ , and equations (51)-(54) for the  $\rho$ 's are decoupled from equations (55), (56), and (57) for the  $\kappa$ 's. This leads to a nonzero solution for the  $\kappa$ 's only in the second order in low frequency amplitude  $g_1$ . Therefore, in this case we have low frequency responses only for the quantities  $\langle \sigma_Z \rangle$  and  $\langle \frac{d\sigma_Z}{dt} \rangle$ , which are given by equations (83) and (88). In the equations for the  $\rho$ 's and  $\chi_\rho$ 's we should substitute  $\gamma B_{LF}$  for  $g_1$ , and  $\gamma$  for  $2\varepsilon/\hbar\Delta_\varepsilon$ , respectively.

The macroscopic magnetic moment of a sample with  $N$  spin-1/2 particles is as follows:

$$M_Z = \frac{N\gamma\hbar}{2}\langle \sigma_Z \rangle \quad (102)$$

The stationary magnetization  $M_Z^{(ST)}$  is given by the stationary solution of (88) or by the stationary part of (89). By making of the substitutions  $\Gamma_\varphi = 1/T_2$ ,  $\Omega_1 = \gamma B_1$ ,  $\Delta_\varepsilon = \hbar\gamma B_0$ , we obtain for  $M_Z^{(ST)}$  a well known expression<sup>32</sup>:

$$M_Z^{(ST)} = M_0 \frac{1 + (T_2\delta)^2}{1 + (T_2\delta)^2 + T_1 T_2 (\gamma B_1)^2} \quad (103)$$

where

$$M_0 = -\tanh\left(\frac{\hbar\gamma B_0}{2k_B T}\right)$$

According to (83) the low frequency response of  $M_Z(t)$  is

$$M_Z^{(LF)}(t) = \frac{N\gamma\hbar}{2}\left(\rho^{(1)}(t) \cos 2\theta + \rho_+^{(1)}(t) \sin 2\theta\right) \quad (104)$$

where  $\rho^{(1)}(t)$  and  $\rho_+^{(1)}(t)$  can be expressed in terms of the real ( $\chi'$ ) and imaginary ( $\chi''$ ) parts of their corresponding susceptibilities:  $\rho^{(1)}(t) = B_{LF}(\chi'_\rho(\omega) \cos\omega t - \chi''_\rho(\omega) \sin\omega t)$ , and  $\rho_+^{(1)}(t) = B_{LF}(\chi'_{\rho_+}(\omega) \cos\omega t - \chi''_{\rho_+}(\omega) \sin\omega t)$ .

In the same way we obtain from (88) the low frequency response for  $\frac{dM_Z}{dt}$ :

$$\frac{dM_Z^{(LF)}}{dt} = -i\frac{N\gamma\hbar}{2}\Omega_R \sin 2\theta \rho_-^{(1)}(t) - \frac{M_Z^{(LF)}(t)}{T_1} \quad (105)$$

where  $\rho_-^{(1)}(t) = iB_{LF}(\chi'_{\rho_-}(\omega) \sin\omega t + \chi''_{\rho_-}(\omega) \cos\omega t)$ .

The corresponding susceptibilities are given by Eqs. (61), (62), and (63) or for small high frequency detuning ( $\delta \ll \Omega_R$ ) by Eqs.(65), (66), and (67) where we should substitute  $\gamma$  for  $2\varepsilon/\hbar\Delta_\varepsilon$ .

The current state of the art allows one to detect low frequency oscillations either of  $M_Z$  with the help of superconducting quantum interference devices (SQUIDS)<sup>33,34</sup> or of  $dM_Z/dt$  by a high quality resonant tank circuit<sup>35</sup>. Below we write down the explicit form of  $M_Z^{(LF)}(t)$  for the case of small high frequency detuning ( $\delta \ll \Omega_R$ ). In this case the susceptibilities are as follows:

$$\chi_\rho(\omega) = -\frac{\gamma\Omega_R}{\Gamma_\varphi} \frac{\rho_+^{(0)}}{i\omega + \Gamma_\varphi} \quad (106)$$

$$\chi_{\rho_+}(\omega) = -\delta\gamma \frac{\rho_+^{(0)}}{\Gamma_\varphi d(\omega)} \left[ i\omega + \frac{1}{T_1} - \frac{\Omega_R^2}{\Gamma_\varphi} \right] \quad (107)$$

$$\chi_{\rho_-}(\omega) = i\delta\gamma \frac{\Omega_R \rho_+^{(0)}}{\Gamma_\varphi^2 d(\omega)} \frac{\left(i\omega + \frac{1}{T_1}\right)(i\omega + 2\Gamma_\varphi)}{(i\omega + \Gamma_\varphi)} \quad (108)$$

where  $d(\omega)$  is defined in (68),  $\Omega_R = \gamma B_1$ , and

$$\rho_+^{(0)} = \frac{\Gamma_\varphi}{\Gamma_\varphi + \gamma^2 B_1^2 T_1} \tanh\left(\frac{\hbar\gamma B_0}{2k_B T}\right) \quad (109)$$

For  $M_Z^{(LF)}(t)$  we obtain:

$$M_Z^{(LF)}(t) = \frac{N\hbar\gamma}{2}(\gamma B_{LF}) \delta \frac{\Omega_R^2}{\Gamma_\varphi^2} \rho_+^{(0)} \times [A_Z(\omega) \cos\omega t + B_Z(\omega) \sin\omega t] \quad (110)$$

where

$$A_Z(\omega) = \frac{\left[ \omega^4 - \omega^2 (\Omega_R^2 - 3\Gamma_\varphi^2) - 2\Gamma_\varphi^2 \left( \Omega_R^2 + \frac{\Gamma_\varphi}{T_1} \right) \right]}{(\omega^2 + \Gamma_\varphi^2) \left[ \left( \tilde{\Omega}_R^2 - \omega^2 \right)^2 + \omega^2 (\Gamma_\varphi + T_1^{-1})^2 \right]} \quad (111)$$

$$B_Z(\omega) = \frac{\omega}{T_1} \frac{\left[ \omega^2 + \Gamma_\varphi T_1 \left( \Omega_R^2 + \frac{\Gamma_\varphi}{T_1} + 2\Gamma_\varphi^2 \right) \right]}{(\omega^2 + \Gamma_\varphi^2) \left[ \left( \tilde{\Omega}_R^2 - \omega^2 \right)^2 + \omega^2 (\Gamma_\varphi + T_1^{-1})^2 \right]} \quad (112)$$

$$\tilde{\Omega}_R^2 = \Omega_R^2 + \Gamma_\varphi/T_1.$$

### VIII. CONCLUSION

In this paper in the frame of the dressed state approach we have analyzed the interaction of a dissipative two level quantum system with high and low frequency excitations. We have found a linear response of the cou-

pled TLS and associated photon field system to a signal whose frequency is of the order of the Rabi frequency. The response of the system exhibits an undamped low frequency oscillation, whose amplitude has a clear resonance at the Rabi frequency with the width being dependent on the damping rates of the system. The explicit expressions for low frequency susceptibility of the TLS, which we obtained in the paper, have a rather general nature and can be applied for the investigation of specific physical systems. As an illustration of our approach we study in detail two rather different physical systems: the flux qubit and real spin under NMR conditions.

### Acknowledgments

The author thanks Evgeni Ilichev for many stimulating discussions. The financial support from the ESF under grant No. 1030 and DFG under grant IL 150/1-1 as well as the hospitality of IPHT (Jena, Germany) is greatly acknowledged.

---

## Appendix

### A. Calculation of matrix elements of $\hat{L}$ in the dressed state basis

With the aid of (9), (10) and (24), we obtain for  $\langle 1, N | \hat{L} | 1, N \rangle$ :

$$\begin{aligned} \langle 1, N | \hat{L} | 1, N \rangle = & \sin^2 \theta \langle a, N | \hat{L} | a, N \rangle + \cos^2 \theta \langle b, N - 1 | \hat{L} | b, N - 1 \rangle + \sin \theta \cos \theta \left[ \langle a, N | \hat{L} | b, N - 1 \rangle + \langle b, N - 1 | \hat{L} | a, N \rangle \right] = \\ & \sin^2 \theta [-\Gamma_\uparrow \langle a, N | \sigma | a, N \rangle + \Gamma_\downarrow \langle b, N | \sigma | b, N \rangle] + \cos^2 \theta [-\Gamma_\downarrow \langle b, N - 1 | \sigma | b, N - 1 \rangle + \Gamma_\uparrow \langle a, N - 1 | \sigma | a, N - 1 \rangle] - \\ & \Gamma_\varphi \sin \theta \cos \theta [\langle a, N | \sigma | b, N - 1 \rangle + \langle b, N - 1 | \sigma | a, N \rangle] \quad (113) \end{aligned}$$

Further transformation requires the substitution of the uncoupled states in (113) with the dressed states by using Eqs. (11), and (12). As a result we obtain:

$$\begin{aligned} \langle 1, N | \hat{L} | 1, N \rangle = & - \langle 1, N | \sigma | 1, N \rangle [\Gamma_\uparrow \sin^4 \theta + \Gamma_\downarrow \cos^4 \theta + 2\Gamma_\varphi \sin^2 \theta \cos^2 \theta] - \langle 2, N | \sigma | 2, N \rangle \sin^2 \theta \cos^2 \theta [\Gamma_\uparrow + \Gamma_\downarrow - 2\Gamma_\varphi] + \\ & [\langle 1, N | \sigma | 2, N \rangle + \langle 2, N | \sigma | 1, N \rangle] \sin \theta \cos \theta [\Gamma_\uparrow \sin^2 \theta - \Gamma_\downarrow \cos^2 \theta + \Gamma_\varphi \cos 2\theta] + \sin^2 \theta \cos^2 \theta \Gamma_\downarrow \langle 1, N + 1 | \sigma | 1, N + 1 \rangle + \\ & \sin^2 \theta \cos^2 \theta \Gamma_\uparrow \langle 1, N - 1 | \sigma | 1, N - 1 \rangle + \sin^4 \theta \Gamma_\downarrow \langle 2, N + 1 | \sigma | 2, N + 1 \rangle + \cos^4 \theta \Gamma_\uparrow \langle 2, N - 1 | \sigma | 2, N - 1 \rangle + \\ & [\langle 1, N + 1 | \sigma | 2, N + 1 \rangle + \langle 2, N + 1 | \sigma | 1, N + 1 \rangle] \Gamma_\downarrow \sin^3 \theta \cos \theta - \\ & [\langle 1, N - 1 | \sigma | 2, N - 1 \rangle + \langle 2, N - 1 | \sigma | 1, N - 1 \rangle] \Gamma_\uparrow \sin \theta \cos^3 \theta \quad (114) \end{aligned}$$

We do not explicitly write here the other matrix elements of  $\hat{L}$ , such as  $\langle 2, N | \hat{L} | 2, N \rangle$ ,  $\langle 1, N | \hat{L} | 2, N \rangle$ ,  $\langle 1, N | \hat{L} | 1, N - 1 \rangle$ ,  $\langle 2, N | \hat{L} | 2, N - 1 \rangle$ ,  $\langle 1, N | \hat{L} | 2, N - 1 \rangle$ ,  $\langle 2, N | \hat{L} | 1, N - 1 \rangle$ , which can be obtained by similar procedure.

**B. Calculations of the averages of Pauli spin operators  $\langle\sigma_X\rangle$ ,  $\langle\sigma_Y\rangle$ , and  $\langle\sigma_Z\rangle$  in the dressed state basis**

$$\begin{aligned} \langle\sigma_Z\rangle = Tr(\sigma\sigma_Z) &= \sum_N \langle 1, N | \sigma\sigma_Z | 1, N \rangle + \sum_N \langle 2, N | \sigma\sigma_Z | 2, N \rangle = \sum_N \langle 1, N | \sigma | 1, N \rangle \langle 1, N | \sigma_Z | 1, N \rangle + \\ &\sum_N \langle 1, N | \sigma | 2, N \rangle \langle 2, N | \sigma_Z | 1, N \rangle + \sum_N \langle 2, N | \sigma | 1, N \rangle \langle 1, N | \sigma_Z | 2, N \rangle + \sum_N \langle 2, N | \sigma | 2, N \rangle \langle 2, N | \sigma_Z | 2, N \rangle \end{aligned} \quad (115)$$

$$\begin{aligned} \langle\sigma_i\rangle = Tr(\sigma\sigma_i) &= \sum_N \langle 1, N | \sigma\sigma_i | 1, N \rangle + \sum_N \langle 2, N | \sigma\sigma_i | 2, N \rangle = \\ &\sum_N \langle 1, N | \sigma | 1, N+1 \rangle \langle 1, N+1 | \sigma_i | 1, N \rangle + \sum_N \langle 1, N | \sigma | 1, N-1 \rangle \langle 1, N-1 | \sigma_i | 1, N \rangle + \\ &\sum_N \langle 1, N | \sigma | 2, N+1 \rangle \langle 2, N+1 | \sigma_i | 1, N \rangle + \sum_N \langle 1, N | \sigma | 2, N-1 \rangle \langle 2, N-1 | \sigma_i | 1, N \rangle + \\ &\sum_N \langle 2, N | \sigma | 1, N+1 \rangle \langle 1, N+1 | \sigma_i | 2, N \rangle + \sum_N \langle 2, N | \sigma | 1, N-1 \rangle \langle 1, N-1 | \sigma_i | 2, N \rangle + \\ &\sum_N \langle 2, N | \sigma | 2, N+1 \rangle \langle 2, N+1 | \sigma_i | 2, N \rangle + \sum_N \langle 2, N | \sigma | 2, N-1 \rangle \langle 2, N-1 | \sigma_i | 2, N \rangle \end{aligned} \quad (116)$$

where  $i = X, Y$ .

- 
- <sup>1</sup> I. I. Rabi, Phys. Rev. **51**, 652 (1937).  
<sup>2</sup> Atomic and Molecular Beams: The State of The Art 2000, (Roger Compargue, ed.) Springer Verlag Telos, 2001.  
<sup>3</sup> J. M. Raimond, M. Brune, and S. Haroche, Rev. Mod. Phys. **73**, 565 (2001).  
<sup>4</sup> Makhlin Y. Schön G. and Shnirman A., Rev. Mod. Phys., **73** (2001) 357.  
<sup>5</sup> D. V. Averin, in: *Exploring the quantum/classical frontier: recent advances in macroscopic quantum phenomena*, Ed. by J.R. Friedman and S. Han, (Nova Publishes, Hauppauge, NY, 2002), p. 441; cond-mat/0004364.  
<sup>6</sup> A.N. Korotkov and D.V. Averin, Phys. Rev. B **64**, 165310 (2001).  
<sup>7</sup> A.N. Korotkov, Phys. Rev. B **63**, 115403 (2001).  
<sup>8</sup> Y. Nakamura, Yu. A. Pashkin, and J. S. Tsai, Phys. Rev. Lett. **87**, 246601 (2001).  
<sup>9</sup> D. Vion, A. Aassime, A. Cottet, P. Joyez, H. Pothier, C. Urbina, D. Esteve, M. H. Devoret, Science **296**, 886 (2002).  
<sup>10</sup> J.M. Martinis, S. Nam, J. Aumentado, C. Urbina, Phys. Rev. Lett. **89**, 117901 (2002).  
<sup>11</sup> I. Chiorescu, Y. Nakamura, C. J. P. M. Harmans, and J. E. Mooij, Science **299**, 1869 (2003).  
<sup>12</sup> E. Ilichev, A.Yu. Smirnov, M. Grajcar, A. Izmalkov, D. Born, N. Oukhanski, Th. Wagner, W. Krech, H.-G. Meyer, and A. Zagoskin, Fizika Nizkikh Temperatur, **30**, 823 (2004).  
<sup>13</sup> E. Ilichev, N. Oukhanski, A. Izmalkov, Th. Wagner, M. Grajcar, H.-G. Meyer, A.Yu. Smirnov, A. Maassen van den Brink, M.H.S. Amin, A.M. Zagoskin, Phys. Rev. Lett. **91**, 097906 (2003).  
<sup>14</sup> A. Yu. Smirnov, Phys. Rev. B **68**, 134514 (2003).  
<sup>15</sup> A. Yu. Smirnov, e-print archive cond-mat/0306004.  
<sup>16</sup> Ju. Hauss, Rabi Spektroskopie an Qubit-Oszillator Systemen, Diploma thesis, Karlsruhe University, 2006.  
<sup>17</sup> Ju. Hauss, A. Fedorov, C. Hutter, A. Shnirman, and G. Schön, e-print archive cond-mat/0701041.  
<sup>18</sup> Ya. S. Greenberg and E. Ilichev, e-print archive quant-ph/0502187.  
<sup>19</sup> Ya. S. Greenberg, E. Ilichev and A. Izmalkov, Europhys. Lett., **72**, 880 (2005)  
<sup>20</sup> C. Coen-Tannoudji, J. Dupont-Rock, G. Grynberg, Atom-Photon Interactions. Basic Principles and Applications. (John Wiley and Sons, 1998).  
<sup>21</sup> Grifoni M. and Hanggi P., Phys. Rep., 304 (1998) 229.  
<sup>22</sup> Frequently, the term "Rabi frequency" is associated with the quantity  $\Omega_1$ . Here we call by this term the quantity  $\Omega_R$ , the frequency with which the population oscillates if the high frequency detuning  $\delta$  is different from zero.  
<sup>23</sup> F. Bloch, Phys. Rev. **105**, 1206 (1957).  
<sup>24</sup> A. G. Redfield, IBM J. Res. Dev. **1**, 19 (1957).  
<sup>25</sup> It is true that if the system is subjected to a strong external driving the  $\Gamma$ 's rates and the corresponding rate equations can be substantially modified<sup>14,26</sup>. However, even in this case the most of experiments can adequately be explained by the Bloch equations with phenomenological  $\Gamma$ 's rates as fitting parameters (see, for example,<sup>27</sup>).  
<sup>26</sup> L. Hartmann, I. Goychuk, M. Grifoni, P. Hanggi, Phys. Rev. E **61**, R4687 (2000).  
<sup>27</sup> S. Saito, M. Thorwart, H. Tanaka, M. Ueda, H. Nakano, K. Semba, and H. Takayanagi, Phys. Rev. Lett. **93**, 037001 (2004).  
<sup>28</sup> J. E. Mooij, T. P. Orlando, L. Levitov, L. Tian, C. H. van

- der Wal, and S. Lloyd, *Science* **285**, 1036 (1999).
- <sup>29</sup> T.P. Orlando, J.E. Mooij, L. Tian, C.H. van der Wal, L. Levitov, S. Lloyd, and J.J. Mazo, *Phys. Rev. B* **60**, 15398 (1999).
- <sup>30</sup> Ya. S. Greenberg, A. Izmalkov, M. Grajcar, E. Ilichev, W. Krech, H.-G. Meyer, M. H. S. Amin, and A. Maassen van den Brink, *Phys. Rev B* **66**, 214525 (2002).
- <sup>31</sup> M. Grajcar, A. Izmalkov, E. Ilichev, Th. Wagner, N. Oukhanski, U. Hubner, T. May, I. Zhilyaev, H. E. Hoenig, Ya. S. Greenberg, V. I. Shnyrkov, D. Born, W. Krech, H.-G. Meyer, A. Maassen van den Brink, and M. H. S. Amin, *Phys. Rev. B* **69**, 060501(R) (2004).
- <sup>32</sup> F. Bloch, *Phys. Rev.* **70**, 460 (1946).
- <sup>33</sup> Ya. S. Greenberg *Rev. Mod. Phys.* **70**, 175 (1998).
- <sup>34</sup> R. McDermot, A. H. Trabesinger, M. Mück, E. L. Hahn, A. Pines, and J. Clarke, *Science* **295**, 2247 (2002).
- <sup>35</sup> S. Appelt, F. W. Häsing, H. Kühn, J. Perlo, and B. Blümich, *Phys. Rev. Lett.* **94**, 197602 (2005).